80th Jubilee
Academician D.Dorjgotov

ENVIRONMENT AND SUSTAINABLE DEVELOPMENT OF THE MONGOLIAN PLATEAU AND SURROUNDING TERRITORIES

XIII INTERNATIONAL CONFERENCE

PROCEEDINGS

ICOMP 2020

2020

CONTENTS

CLASSIFICATION OF FOREST AREA USING OPTICAL AND RADAR IMAGES

Acad. Amarsaikhan D.

1Institute of Geography and Geoecology, Mongolian Academy of Sciences, Ulaanbaatar, Mongolia
2Department of Geography, Mongolian State University of Education, Ulaanbaatar, Mongolia
3Department of Geography, National University of Mongolia, Ulaanbaatar, Mongolia

Co-author: D.Enkhjargal 1, Ts.Bat-Erdene2, G.Tsogzol1, Ch.Bolorchuluun3

Abstract: The aim of this study is to conduct a forest area classification using optical and synthetic aperture radar (SAR) satellite data sets. For this purpose, a forested site around the Lake Khuvsgul situated in northern Mongolia is selected. As remote sensing (RS) data sources, multispectral Landsat 8 images and ALOS-2 PALSAR L-band HH polarization data are used. To produce a reliable land cover map from the combined multichannel and SAR images, a support vector machine (SVM) and maximum likelihood classification (MLC) techniques are compared. For the accuracy assessment, an overall accuracy that applies a confusion matrix is used. Overall, the research demonstrates that the integrated optical and microwave RS can be efficiently used for the forest area discrimination.

Keywords: Optical, Microwave, Forest area, Classification

Introduction

Forest cover occupies a noticeable part of the planet's land area and range from undisturbed primary forests to forests managed and used for a variety of different purposes. Utilization of forest resources has an impact on the environment and on the economies of the world nations (Kangas, 2018). Forests have a history of being exploited either adequately, but more efforts are now being made towards their sustainable use. The assessment of forests in terms of their extent, condition, use and value is periodically realized at both global and national levels. Applications relating to the monitoring of forest status and to forest management require updated and accurate inventories, summarizing information of the changes related to the forests, rates and patterns of deforestation and afforestation (Persson and Stahl, 2020).

Historically, forestry has been concerned mainly with the assessment of timber resources and the management and utilization of closed forests for the production of wood. The applications of satellite data for effective forest management on a more scientific basis is consistent with the priorities set at national, regional, and local level studies. The shift in priority of forest management towards ecologically sustainable forest resources management call for reliable thematic spatial information with a provision to update and retrieve for management decisions at various levels (Barbara, 2016). Sustainable forest management aims to manage forested areas in order to obtain products and services while simultaneously minimizing any undesirable effects on the social and surrounding environments (Fernandez-Ordonez et al. 2009). In other words, it is a balancing act between the demands of an ever increasing human population and maintenance of the ecological functions of healthy forest ecosystems (MacDicken et al. 2015).

Remote sensing is used in a wide array of forestry applications, including forest cover updating, depletion monitoring and measuring, forest type discrimination; determination of biophysical properties of forest stands; collecting harvest information; updating of inventory information for timber supply, biomass estimation, species inventory, regeneration assessment; monitoring the quantity, health and diversity of the forests. In addition, RS techniques can identify, distinguish, classify, assess and measure different timberland attributes both qualitatively and quantitatively (Thilagavathi1 and Nagendran, 2017). The RS of forests has reached a developmental stage that allows practitioners to expend the largest proportion of their efforts on information generation, rather than data preparation (White et al. 2016).

Nowadays there is a great variety of RS data, with a wide range of resolutions and many new types of sensors. Nevertheless, the technology still has not successfully been applied to real forest management at a fully operational level (Bolton et al. 2018). Possible reasons could include operational cost, skilled personnel, lack of technoogy and institutional problems. Applications of RS for forest management should be based on operational knowledge and experience and be embedded in regular management operations. To reach this goal, for many years, optical RS data sets have been used for different forest studies, mainly considering the global and regional mapping (Enkhjargal et al. 2015).

Optical sensors usually use visible and infrared radiation for imaging the forest cover. Over the years, different studies have provided knowledge on how various forest related factors influence the reflectance properties in the visible and infrared portions of electro-magnetic spectrum. In recent years, microwave sensors have been widely used for forest mapping and analysis. The radar instruments image an area not depending on the solar illumination and are not affected by cloudy or rainy conditions like optical sensors. They usually operate in longer wavelengths and provide information on the tree structure of forested areas and suitable for mapping and monitoring over large areas with high to moderate spatial resolutions (Vafaei et al. 2015). Different forest related research based on classification methods have been carried out by combining optical and microwave images, because of their different characteristics. Many of the authors judged that the outputs provide the promising results (Huang et al. 2009, Morel et al. 2012, Amarsaikhan and Ganchuluun, 2015).

The aim of this research is to conduct a forest classification using optical and radar images. For this purpose, a test site located in northern Mongolia has been selected. As RS data sources, multispectral Landsat 8 images and ALOS-2 PALSAR L-band HH polarization data were used. To produce a land cover map from the multisensor images, a SVM and MLC techniques have been used and compared.

Methods, Test Site and Data Sources

In the present study, the research methods include such techniques as geometric correction-georeferencing of the space images, speckle suppression of radar data, SVM, MLC methods. The aim of the geometric correction is to produce a geometrically corrected image with a high level of positional accuracy. In the meantime, the corrected image should be georeferenced to a projected coordinate system. In most cases, the SAR images have a granular appearance due to the speckle formed as a result of the coherent radiation used for radar systems. Therefore, the speckle reduction is a very important step in further analysis in microwave images (Serkan *et al.* 2008, Amarsaikhan *et al.* 2012). The SVM is a classification technique derived from the statistical learning theory. It usually separates the classes with a decision surface that maximizes the margin between the selected classes. The surface is often called the optimal hyper-plane, and the data points closest to the hyperplane are called support vectors (ENVI, 2009). The basis of the MLC are the actual frequencies of co-occurrence between the selected class and observation vectors. The method assumes that the statistics for each class in each band are normally distributed and calculates the probability that a given pixel belongs to a specific class. Unless the user selects a probability threshold, all pixels are classified. Each pixel is assigned to the class that has the highest probability. If the highest probability is smaller than a threshold you specify, the pixel remains unclassified (Nyamjargal et al. 2019).

The test area is located in Khuvsgul aimag of the northern part of Mongolia and it borders with Russian Federation. The aimag is famous with its freshwater and deep lake of Khuvsgul and different mountain ranges, isolated and deep forests and peculiar customs of many ethnic groups. The south and southwest are dominated by the round-topped Tarvagatai, Bulnai and Erchim sub-ranges of the Khangai massif. The areas west and north of Lake Khuvsgul are formed by the alpine Khoridol Saridag, Ulaan Taiga, and Munkh Saridag mountains. The center and east parts are less mountainous, but still hilly. The mountain slopes in the area are clothed with boreal taiga forest. The taiga zone experiences more precipitation and lower temperatures than most of Mongolia, therefore plant growing period is comparatively short. It forms the most southern extension of the east Siberian taiga and consists mainly from larch and pine trees and rich in mosses and lichens. Here are found a great number of medical herbs, such as peony, liquorice, astragalus, wild rose, saussurea involucrata, hawthorn, valerian, thyme, thermopsis (Batsukh, 2008).

Figure 1. Landsat 8 image of the test area (R=B5, G=B4, B=B3).

In the study, as data sources, Landsat 8 data of 03 September 2019 and ALOS-2 PALSAR L-band HH polarization image of 25 July 2018 have been used. The Landsat 8 data has nine reflective bands (B1: 0.43–0.45μm, B2: 0.45–0.51μm, B3: 0.53–0.59μm, B4: 0.64–0.67μm, B5: 0.85–0.88μm, B6: 1.57–1.65μm, B7: 2.11–2.29μm, B8: 0.50–0.61μm and B9: 1.36–1.38μm). The spatial resolution is 30 m for all multispectral bands, but panchromatic band 8 has a spatial resolution of 15 m (Munkhdulam et al. 2019). In the present study, channels 2,3,4,5,6,7 have been used. ALOS-2 PALSAR is the second of the Japanese ALOS Programme satellite and the data has a spatial resolution of 25m. The PALSAR-2 became a unique and highly useful sensor achieving a high resolution, wide swath width and image quality, expanding its transmission power and bandwidth, and adopting new technologies such as dual-beam receivers, complex chirp modulations, and highly efficient data compression (Amarsaikhan et al. 2015). In addition, a topographic map of 1986, scale 1:100,000 and a forest taxonomy map of 1984, scale

1: 500,000 have been used. Figure 1 shows a Landsat 8 image of the test site, and some examples of its land cover.

Results and Discussion

In the beginning, the multispectral Landsat 8 images were geometrically corrected to a UTM map projection using a topographic map of the study area, scale 1:100,000. The ground control point (GCP)s have been selected on clearly delineated sites of the lake corners and other clear sites. In total 15 points were selected. For the transformation, a second order transformation and nearest neighbour resampling approach have been applied and the related root mean square error (RMSE) were 0.98 pixels. In order to geometrically correct the PALSAR image, 16 more regularly distributed GCPs were selected comparing the locations of the selected points with other information such as Landsat ETM+ image, topographic map and forest taxonomy map. Then, the microwave image was georeferenced to a UTM map projection using the selected topographic map of the study area. For the actual transformation, a second order transformation and nearest neighbour resampling approach were applied and the related RMSE was 1.29 pixel. The transformation of the SAR image's RMSE exceeded 1 pixel, because on the selected microwave image it was not easy to determine the exact locations likewise the optical data.

Figure 2. The ALOS-2 PALSAR image of the test area.

Then, in order to reduce the speckle three different speckle suppression techniques such as local region, frost and gammamap filters (ERDAS, 2007) of 3x3 size were applied to the SAR image and compared in terms of delineation of forest and other texture information. After visual inspection of each image, it was found that the selected gammamap filter created the best image in terms of delineation of different features as well as preserving content of texture information. After the speckle suppression, the PALSAR image was added to the optical bands, thus forming multisource data sets. Figure 2 shows a georeferenced SAR image of the test site.

Before applying the decision-rule, in order to define the sites for the training signature selection, several areas of interest (AOI) representing the selected classes (i.e., coniferous forest, deciduous forest, grassland, light soil, dark soil and water) have been selected. As the data sources included both optical and SAR features, the fused images were very useful for the determination of the homogeneous AOI as well as for the initial intelligent guess of the training sites. The separability of the training signatures was firstly checked in feature space and then evaluated using JM distance (Mather and Koch, 2010). After the investigation, the samples that demonstrated the greatest separability were chosen to form the final signatures. The final signatures included about 614-4071 pixels. For the classification, the following feature combinations were compared:

1. Visible and near infrared bands of Landsat 8 data.
2. All spectral bands of Landsat 8 data.
3. ALOS PALSAR and full Landsat 8 data.

To increase the reliability of the classification, to the initially classified images, a fuzzy convolution with a 3x3 size window was applied. The fuzzy convolution creates a thematic layer by calculating the total weighted inverse distance of all the classes in a determined window of pixels and assigning the centre pixel the class with the largest total inverse distance summed over the entire set of fuzzy classification layers that is classes with a very small distance value will remain unchanged while the classes with higher distance values might change to a neighboring value if there are a sufficient number of neighboring pixels with class values and small corresponding distance values (ERDAS, 2007).

The visual inspection of the fuzzy convolved images indicated that there are some improvements on the borders of the neighboring classes that significantly influence the separation of the decision boundaries in multidimensional feature space. The final classified images using both SVM and MLC are shown in Figure 3(a–f). As seen from the Figure 3(a–c), the classification results of the original Landsat bands give the worst results, because there are high overlaps among grassland and forest classes. However, these overlaps decrease on other images for the classification of which SAR and optical bands have been used.

For the accuracy assessment of the classification results, the overall performance has been used. This approach creates a confusion matrix in which reference pixels are compared with the classified pixels and as a result an accuracy report is generated indicating the percentages of the overall accuracy (Amarsaikhan *et al.* 2012). As ground truth information, different AOIs containing 5,879 purest pixels have been selected. AOIs were selected on a principle that more pixels to be selected for the evaluation of the larger classes such as grassland and coniferous forest than the smaller classes such as deciduous forest and dark soil. The overall classification accuracies for the selected classes in different band combinations are shown in Table 1. From the Table 1, it is seen that the performance of the combined use of optical and SAR data sets was better that the other combinations.

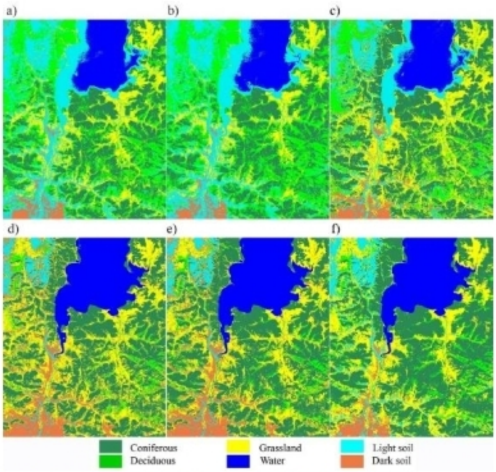

Figure 3. Comparison of the classification results for the selected classes:
(a) MLC image using vis/NIR bands of Landsat 8,
(b) MLC image using all spectral bands of Landsat 8,
(c) MLC image using SAR and Landsat 8,
(d) SVM classified image using vis/NIR bands of Landsat 8,
(e) SVM classified image using all spectral bands of Landsat 8,
(f) SVM classified image using SAR and Landsat 8.

Before applying the decision-rule, in order to define the sites for the training signature selection, several areas of interest (AOI) representing the selected classes (i.e., coniferous forest, deciduous forest, grassland, light soil, dark soil and water) have been selected. As the data sources included both optical and SAR features, the fused images were very useful for the determination of the homogeneous AOI as well as for the initial intelligent guess of the training sites. The separability of the training signatures was firstly checked in feature space and then evaluated using JM distance (Mather and Koch, 2010). After the investigation, the samples that demonstrated the greatest separability were chosen to form the final signatures. The final signatures included about 614-4071 pixels. For the classification, the following feature combinations were compared:

1. Visible and near infrared bands of Landsat 8 data.
2. All spectral bands of Landsat 8 data.
3. ALOS PALSAR and full Landsat 8 data.

To increase the reliability of the classification, to the initially classified images, a fuzzy convolution with a 3x3 size window was applied. The fuzzy convolution creates a thematic layer by calculating the total weighted inverse distance of all the classes in a determined window of pixels and assigning the centre pixel the class with the largest total inverse distance summed over the entire set of fuzzy classification layers that is classes with a very small distance value will remain unchanged while the classes with higher distance values might change to a neighboring value if there are a sufficient number of neighboring pixels with class values and small corresponding distance values (ERDAS, 2007).

The visual inspection of the fuzzy convolved images indicated that there are some improvements on the borders of the neighboring classes that significantly influence the separation of the decision boundaries in multidimensional feature space. The final classified images using both SVM and MLC are shown in Figure 3(a–f). As seen from the Figure 3(a–c), the classification results of the original Landsat bands give the worst results, because there are high overlaps among grassland and forest classes. However, these overlaps decrease on other images for the classification of which SAR and optical bands have been used.

For the accuracy assessment of the classification results, the overall performance has been used. This approach creates a confusion matrix in which reference pixels are compared with the classified pixels and as a result an accuracy report is generated indicating the percentages of the overall accuracy (Amarsaikhan *et al.* 2012). As ground truth information, different AOIs containing 5,879 purest pixels have been selected. AOIs were selected on a principle that more pixels to be selected for the evaluation of the larger classes such as grassland and coniferous forest than the smaller classes such as deciduous forest and dark soil. The overall classification accuracies for the selected classes in different band combinations are shown in Table 1. From the Table 1, it is seen that the performance of the combined use of optical and SAR data sets was better that the other combinations.

Table 1. Classification accuracies.

Feature combinations	Overall accuracy
MLC (Landsat-Vis/NIR)	78.09
MLC (Landsat-All bands)	79.98
MLC (Landsat-PALSAR)	82.18
SVM(Landsat-Vis/NIR)	88.05
SVM(Landsat-All bands)	89.74
SVM(Landsat-PALSAR)	93.61

Conclusions

The aim of this study was to conduct a classification of the forest site in Khuvsgul area, northern Mongolia using refined spatial features. As data sources, multispectral Landsat 8 images, ALOS-2 PALSAR L-band HH polarization data, a topographic map, and a forest taxonomy map were used. To produce the updated land cover map from the multisensor images, the SVM and MLC techniques were compared. As could be seen from the overall classification results, the combined application of optical and SAR data sets produced a better result than the single source image. Moreover, it was seen that the performance of the SVM was better than the performance of the MLC. Overall, the study demonstrated that the advanced optical and microwave RS could be reliable tools for forest planning and management.

References

Amarsaikhan, D., Saandar, M., Ganzorig, M., Blotevogel, H.H. and Enkhjargal, D., 2012. Comparison of multisource image fusion methods and land cover classification. *International Journal of Remote Sensing*, 33(8), pp. 2532-2550.

Amarsaikhan, D. and Ganchuluun, N., 2015. CHAPTER 4 –“Fusion and Classification of Multisource Images for Update of Forest GIS” in “IMAGE FUSION: PRINCIPLES, TECHNOLOGY AND APPLICATIONS” BOOK published by Nova Science Publishers, New York, USA, pp.83-121.

Amarsaikhan, D., Battsengel, V., Bolor, G., Enkhjargal, D. and Jargaldalai, E., 2015. Fusion of optical and SAR images for enhancement of forest classes, Full paper published in CD-ROM Proceedings of the ACRS, Manila, Philippines.

Barbara, K., 2016. "Remote sensing supporting national forest assessments." *Faculty of Forest and Environmental Science,* University of Freiburg, Stьhlingen.

Batsukh, N. 2008. *Mongolian Forest Ecosystems*, Ulaanbaatar: World Wildlife Fund, Ulaanbaatar, Mongolia.

Bolton, D.K.; White, J.C.;Wulder, M.A.; Coops, N.C.; Hermosilla, T.; Yuan, X. 2018, Updating stand-level forest inventories using airborne laser scanning and Landsat time series data. Int. J. Appl. Earth Obs. Geoinf. 66, 174–183.

Enkhjargal, D., Amarsaikhan, D., Bolor, G., Tsetsegjargal, N. and Tsogzol, G., 2015. Forest mapping in Mongolia using optical and SAR images, Full paper published in CD-ROM Proceedings of the ACRS, Manila, Philippines.

ENVI, 2009. ENVI User's Guide, Version 4.7 Edition.

ERDAS, 2009. ERDAS Field Guide, Atlanta, Georgia.

Fernandez-Ordonez, Y., Soria-Ruiz, J. and Leblon, B., 2009. Forest Inventory using Optical and Radar Remote Sensing, Advances in Geoscience and Remote Sensing, Gary Jedlovec (Ed.), ISBN: 978-953-307-005-6, Intech Open Access.

Huang, Sh., Crabtree, R. L., Potter, Ch. and Gross, P. 2009. Estimating the quantity and quality of coarse woody debris in Yellowstone post-fire forest ecosystem from fusion of SAR and optical data. *Remote Sensing of Environment*, Vol.113(9), pp.1926-1938.

Kangas AS, Astrup R, Breidenbach J, Fridman J, Gobakken T, Korhonen KT, Maltamo M, Nilsson M, Nord-Larsen T, Nжsset E, Olsson H. 2018. Remote sensing and forest inventories in Nordic countries – roadmap for the future. Scand J For Res. 33:397–412.

MacDicken, K.G., Sola, P., Hall, J.E., Sabogal, C., Tadoum, M., and de Wasseige, C. 2015. "Global progress toward sustainable forest management." *Forest Ecology and Management*, Vol. 352: pp. 47–56.

Morel, A. C., Fisher, J. B. and Malhi, Y. 2012. Evaluating the potential to monitor aboveground biomass in forest and oil palm in Sabah, Malaysia, for 2000-2008 with Landsat ETM+ and ALOS-PALSAR. Vol.33(11), pp. 3614-3639.

Munkhdulam, O., Atzberger, C., Chambers, J. and Amarsaikhan, D., 2018. Mapping pasture biomass in Mongolia using Partial Least Squares, Random Forest regression and Landsat 8 imagery, *International Journal of Remote Sensing,* https://doi.org/10.1080/01431161.201 8.1541110.

Nyamjargal, E., Amarsaikhan, D., Munkh-Erdene, A., Battsengel, V., Bolorchuluun, Ch., 2019. Object-based classification of mixed forest types in Mongolia, *Geocarto International.*

Serkan, M., Musaoglu, N., Kirkici, H. and Ormeci, C., 2008. Edge and fine detail preservation in SAR images through speckle reduction with an adaptive mean filter. *International Journal of Remote Sensing,* 29(23).

Takao, G., Priyadi, G. and Nursal, H., 2010. The operational role of remote sensing in forest and landscape management, Focus group discussion proceedings, Center for International Forestry Research, Japan.

Persson, H. and Stahl, G., 2020. Characterizing Uncertainty in Forest Remote Sensing Studies. Remote Sensing, 12, 505.

Thilagavathi, K. and Nagendran, R., 2017. Remote Sensing Methods for Forestry Applications –A Survey, IJSART - Volume 3 Issue 5, pp.394-398.

Vafaei, S., Soosani, J., Adeli, K.; Fadaei, H., Naghavi, H., Pham, T., 2018. Tien Bui, D. Improving Accuracy
Estimation of Forest Aboveground Biomass Based on Incorporation of ALOS-2 PALSAR-2 and Sentinel-2A
Imagery and Machine Learning: A Case Study of the Hyrcanian Forest Area (Iran). Remote Sens. 10, 172.

White, J. C., N. C. Coops, M. A. Wulder, M. Vastaranta, T. Hilker, and P. Tompalski. 2016. "Remote Sensing Technologies for Enhancing Forest Inventories: A Review." *Canadian Journal of Remote Sensing* 42 (5): 619–641.